

# INTERMEDIATE STRAIN RATE CHARACTERIZATION OF MATERIALS USING A HIGH SPEED SERVO-HYDRAULIC LOAD FRAME

Naftel, A<sup>1\*</sup>, Rahmat, M<sup>1</sup>

<sup>1</sup> Aerospace, National Research Council Canada, Ottawa, Canada

\* Corresponding author ([John.Naftel@nrc-cnrc.gc.ca](mailto:John.Naftel@nrc-cnrc.gc.ca))

**Keywords:** *Dynamic characterization, Strain rate, Servo-hydraulic load frame*

## ABSTRACT

The investigation of material behaviour at intermediate strain rates has become essential as structural materials have become increasingly relied upon in dynamic applications, and many of these materials exhibit strain rate dependent behaviour. The term, “intermediate strain rate” refers to strain rates in the range of 1 to 100 s<sup>-1</sup>, a common example of which would be the strain rates seen in many structural components during a car crash. However, the literature shows a lack of comprehensive datasets for materials tested at intermediate strain rates due to limited access to high speed load frames, in addition to complications in the testing method and data analysis, such as issues related to minimizing the ringing effect commonly seen within the data in these types of tests. This ringing effect is caused by the dynamic waves in the load sensing instrument and appears as large oscillations in the load data.

This paper discusses the testing and analysis procedures developed for intermediate strain rate characterization of a variety of materials including steel, aluminum and epoxy, as well as tests performed at elevated temperatures using a high speed servo-hydraulic load frame. Furthermore, the paper introduces a new material model to accurately represent dynamic stress-strain curves. Lastly, the results of dynamic tests are presented to showcase the capabilities of intermediate strain rate testing using a high speed servo-hydraulic load frame.

## 1 INTRODUCTION

The majority of engineering material data that exists today is for materials which are tested quasi-statically. This is done because quasi-static tests are slow and thus are easily controlled and data easily collected. Additionally, most engineering materials are put to use in structures that are loaded gradually and are not expected to undergo large amounts of strain. However, for applications in which large loads can be expected to be applied quickly, these quasi-static properties no longer represent the physics of the situation and become inaccurate. This occurs as many materials exhibit strain rate dependent behaviour [1-3]. For example, numerous studies have shown that the properties of epoxy composites are affected by strain rate [4-8]. Additionally, both steel and aluminum have been investigated at intermediate strain rates and have been shown to be sensitive to strain rate changes [3, 9, 10]. Many dynamic test methods have been previously developed, from which the split Hopkinson bar testing has become a common test method to determine material properties at high strain rates, when stress waves must be considered in the data analysis [11]. Intermediate strain rate tests, between 1 and 100 s<sup>-1</sup>, are typically carried out with servo-hydraulic high speed test frames [11]. Yet complexities arising from the ringing effect as well as the limited availability of high speed load frames, has led to insufficient intermediate strain rate test data [11-13].

# INTERMEDIATE STRAIN RATE CHARACTERIZATION OF MATERIALS USING A HIGH SPEED SERVO-HYDRAULIC LOAD FRAME

To address the existing gap in datasets of material properties at intermediate strain rates, the National Research Council Canada (NRC) procured a nation-wide unique high speed servo-hydraulic load frame from MTS Systems Corporation. This paper discusses the testing and analysis procedures developed for intermediate strain rate characterization of a variety of materials including steel, aluminum and epoxy, as well as tests performed at elevated temperatures. Moreover, a new material model is presented and fitted to the dynamic stress-strain curves of the materials. Ultimately, the potential of using a high speed servo-hydraulic load frame for intermediate strain rate testing is demonstrated through the presentation of the results.

## 2 METHODS AND ANALYSIS

### 2.1 Test Setup

The tests, conducted using the load frame at NRC, focused on the intermediate range of strain rates for which stress wave propagation can be ignored [11]. However, oscillations in the results, called ringing, are caused by the quick application of the load to the piezoelectric force link, which cause it to act similar to a spring, thus causing oscillations in the force readouts. Therefore, a strain gauge was mounted on the specimen and force values were calculated using the strain gauge data, thus bypassing the force link and avoiding the vibrations in the force link completely. It was noted that the tab sections of the specimens remain in the elastic regime throughout the test. Therefore, strain gauges applied to the tab section allowed strain data to be recorded and converted to force by linear Hooke's law. Figure 1 depicts the measurements from the force link compared to the strain gauge data.

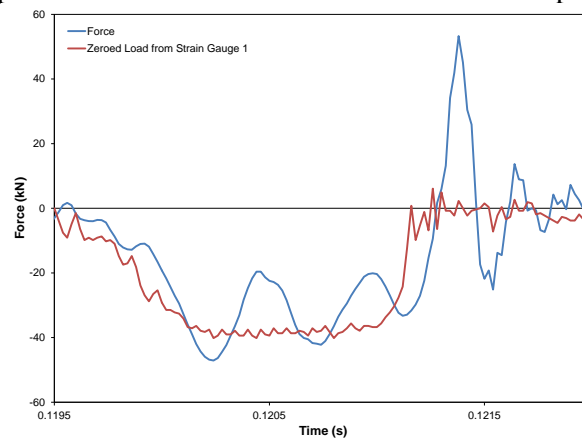


Figure 1: Force link data and the force calculated from strain measurements at the tab section of a steel specimen

It is apparent from the figure that the strain gauge data contains far less oscillations than the force link data. Additionally it can be seen that the force link data lag behind the strain gauge data. This is due to the time it takes for the load to reach the strain gauge, located on the tab section near the site of load application, compared to reaching the force link, located at a farther distance from load application.

The nominal strain rate applied to a specimen is inversely proportional to its gauge length. In this way, due to the small size of the epoxy specimens, head velocities of up to only 2 m/s were required to achieve the desired strain rates for the tests. It was observed that at velocities of 2 m/s and below for this material, the ringing in the force link became insignificant and the force link data were seen to match the strain gauge data, with the exception of the time lag. Therefore, it was decided not to use strain gauges on the epoxy specimens and instead rely solely on the force link data.

# INTERMEDIATE STRAIN RATE CHARACTERIZATION OF MATERIALS USING A HIGH SPEED SERVO-HYDRAULIC LOAD FRAME

## 2.2 Data Analysis

As explained previously, the tab section of the specimen remains in the elastic regime, therefore for materials that show insignificant dependence of tensile Young's modulus on strain rate, the force can be calculated from the strain gauge data through the following equation:

$$F = E\varepsilon A \quad (1)$$

where  $E$  is the tensile Young's modulus of the material,  $\varepsilon$  is the strain gauge readout, and  $A$  is the cross-sectional area on which the strain gauge is mounted [3]. Please note that for the epoxy specimens the force data was taken directly from the force link and this equation was not used.

The start and end of the test were determined through visual inspection of the load-time response graph and both the load and displacement were zeroed at the determined starting point. Before testing, the nominal strain rate can be calculated by dividing the velocity at which the test will take place by the length of the specimen between the grips of the machine. This gives an average strain rate for the entire specimen whereas in reality the strain rate in the gauge section is higher than the average for the specimen. Therefore, after the test is finished the actual strain rate can be determined by dividing the failure strain at the gauge section by the duration of the test.

The velocity of the head was seen to maintain a near constant value throughout the duration of each test, however small deviations from the command signal led to a small noise level in the displacement data. Equation 2 was used to smooth the displacement data without affecting the overall trend.

$$d_i = x_{i-1} + \frac{\sum_{i=1}^{i+199} (x_{i+1} - x_i)}{200} \quad (2)$$

where  $d$  is the smoothed displacement, and  $x$  is the original displacement. The engineering stress  $\sigma_E$  in the gauge section can be calculated by dividing the load by the initial cross-sectional area of the specimen in the gauge section, as shown in equation 3

$$\sigma_{gauge} = \frac{P}{A_{gauge}} \quad (3)$$

where  $P$  is the load, and  $A$  is the initial cross-sectional area of the specimen. Furthermore, knowing the strain in the tab section, the length of the tab section, and the fact that the tab section remains elastic throughout the test, the deformation of the tab section (on both sides of the gauge section) can also be calculated. Additionally, the entire deformation of the specimen (two tab sections and the gauge section) is known based on the head movement. Therefore, by subtracting the deformation occurring in the tab sections from the entire deformation of the specimen, an approximation for the average deformation of the gauge section is obtained through equation 4

$$d_{gauge} = d - 2 \frac{Fl_{tab}}{EA_{tab}} \quad (4)$$

where  $d_{gauge}$  is the displacement in the gauge section,  $l_{tab}$  is the length of the tab section,  $l_{gauge}$  is the length of the gauge section,  $A_{tab}$  is the cross-sectional area of the tab section, and  $E$  is the Young's modulus of the material. Finally, by dividing the deformation of the gauge section by the initial length of the gauge section, the average engineering strain in the gauge section,  $\varepsilon_{gauge}$ , is obtained [3];

$$\varepsilon_{gauge} = \frac{d_{gauge}}{l_{gauge}} \quad (5)$$

## INTERMEDIATE STRAIN RATE CHARACTERIZATION OF MATERIALS USING A HIGH SPEED SERVO-HYDRAULIC LOAD FRAME

It is important to note that this approach does not consider the complex nature of strain distribution during necking. The true stress  $\sigma_T$ , and true strain  $\varepsilon_T$ , are calculated from:

$$\sigma_T = \sigma_{gauge}(1 + \varepsilon_{gauge}) \quad (6)$$

$$\varepsilon_T = \ln(1 + \varepsilon_{gauge}) \quad (7)$$

For materials that show modulus strain rate-independent behaviour, the Young's modulus can then be calculated from the true stress-strain curve by finding the slope of the linear section. For the epoxy specimens the dynamic Young's modulus is significantly different than the quasi-static modulus which was used in force calculation. In order to overcome this issue an iterative approach was adopted. The process started by using the quasi-static modulus to calculate the strain in the tabs, and consequently the strain at the gauge section. With these strains the true stress-strain curves were drawn and the dynamic Young's modulus was calculated from the curve. In the next iteration, the gauge section strain was recalculated using the average of the two moduli that were input and output from the previous iteration, which for the first step were the quasi-static and first dynamic moduli. In order to output a new modulus, the true stress and true strain were then recalculated for each iteration. Using this approach the modulus was seen to have converged to within 5 MPa, for each test after seven iterations. A graph showing every iteration for a 1 m/s dynamic test on epoxy can be seen in Figure 2. The highlighted elastic region shown in the figure indicates the range of data points that were used in the calculation of the modulus.

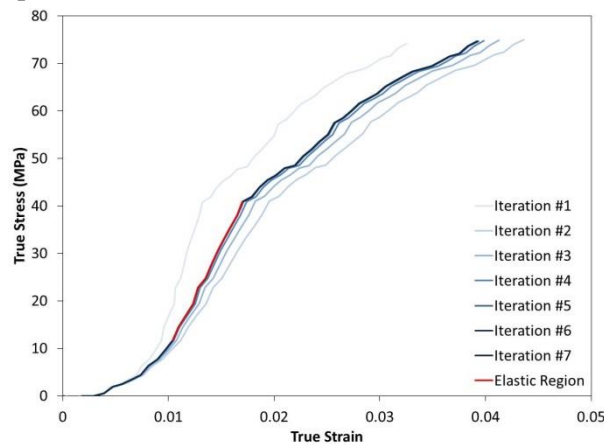


Figure 2: Convergence of stress-strain curves through the iteration of Young's modulus for epoxy

Following the determination of the modulus and the production of the true stress-strain curve, the toe compensation process [14] was performed by shifting each true stress-strain curve along the strain axis so that the linear section from which the modulus was calculated would pass through the origin. Using the true stress-strain curves for each test, all the test data was grouped by strain rate. The data for each individual strain rate was then used to create a single stress-strain curve simultaneously representing the results of all tests conducted at a given strain rate. Data points that represented outliers were eliminated in order to decrease the noise in the data and to increase the readability of the graphs. An example of one of these combined stress-strain curves is shown in Figure 3.

## INTERMEDIATE STRAIN RATE CHARACTERIZATION OF MATERIALS USING A HIGH SPEED SERVO-HYDRAULIC LOAD FRAME

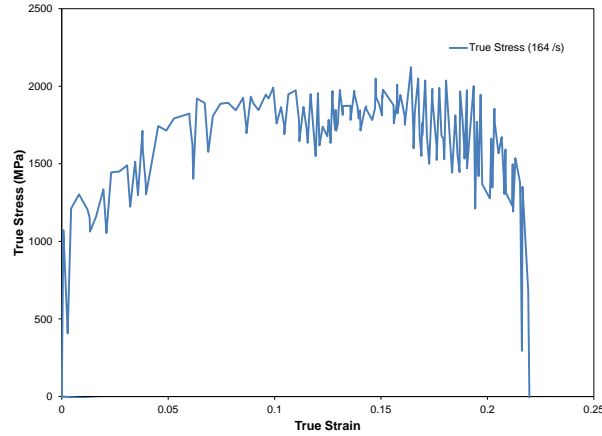


Figure 3: True stress-strain curve for steel tested at a strain rate of  $164 \text{ s}^{-1}$

Finally, ultimate tensile strength and failure strain were read from the curves and the fracture energy was calculated through the integration of the area under the stress-strain curve.

### 2.3 Modified Johnson-Cook Model

The behaviour of material systems under dynamic loading can be described by a range of different material models. Among these semi-empirical models, the one developed by Johnson and Cook (Johnson-Cook model) is perhaps the most widely used [15]. This model includes five material constants (i.e. curve fitting parameters) and considers strain rate hardening and thermal softening effects. The Johnson-Cook model is mathematically expressed as:

$$\sigma = (A + B\varepsilon^n)(1 + C \ln \dot{\varepsilon}^*)(1 - (T^*)^m) \quad (9)$$

where  $\sigma$  is the equivalent stress,  $\varepsilon$  is the equivalent plastic strain,  $\dot{\varepsilon}^* = \dot{\varepsilon}/\dot{\varepsilon}_0$  is the equivalent strain rate, and  $\dot{\varepsilon}_0$  is the reference strain rate.  $T^*$  is calculated from

$$T^* = \frac{T - T_r}{T_m - T_r} \quad (10)$$

in which  $T_r$  is the room temperature, and  $T_m$  is the melting point of the material. In the Johnson-Cook model  $A, B, n, C$ , and  $m$  are material parameters that are obtained from fitting stress-strain curves under different conditions [16].

A least squares regression was performed to fit Johnson-Cook models to the stress-strain curves for the steel and aluminum specimens. The average least squares error was used in the regression, opposed to the total error, so that the curve would not be skewed toward trials where more data points were available. The Johnson-Cook model assumes a sudden failure and is incapable of predicting the gradual failure that is actually seen in the material [17]. Therefore, a modified Johnson-Cook model was developed to fit the stress-strain relationship for the material. The modified Johnson-Cook model is capable of predicting the gradual failure seen in the material. It can mathematically be expressed as:

## INTERMEDIATE STRAIN RATE CHARACTERIZATION OF MATERIALS USING A HIGH SPEED SERVO-HYDRAULIC LOAD FRAME

$$\sigma = \left( A + B \left( \frac{\varepsilon}{1 + E \ln \frac{\dot{\varepsilon}}{\dot{\varepsilon}_0}} \right)^n + D \left( \frac{\varepsilon}{1 + E \ln \frac{\dot{\varepsilon}}{\dot{\varepsilon}_0}} \right)^p \right) \left( 1 + C \ln \frac{\dot{\varepsilon}}{\dot{\varepsilon}_0} \right) (1 - (T^*)^m) \quad (11)$$

where  $\sigma$  is the equivalent stress,  $\varepsilon$  is the equivalent plastic strain,  $\dot{\varepsilon}_0$  is the reference strain rate, and  $A$ ,  $B$ ,  $C$ ,  $D$ , and  $E$  as well as  $n$ ,  $m$  and  $p$  are curve-fitting parameters. This model can be applied for materials that show increase in elongation at failure with increasing strain rate. If the material becomes more brittle with increasing strain rate the term  $1 + E \ln \frac{\dot{\varepsilon}}{\dot{\varepsilon}_0}$  comes to the numerator of the fraction to predict the material behaviour correctly [3]. Following the same least squares procedure used for the Johnson-Cook model, the modified Johnson-Cook model was fitted to the steel data as well as for aluminum specimens, including those tested at an elevated temperature of 100°C.

### 3 RESULTS

#### 3.1 Steel

Algotuf 400 steel dogbone specimens were tested at strain rates ranging from quasi-static ( $2.6 \times 10^{-4} \text{ s}^{-1}$ ) to dynamic ( $189 \text{ s}^{-1}$ ). The results of the steel tests with the Johnson-Cook curve fits are shown in Figure 4 (a) while the modified Johnson-Cook curve fits are shown in Figure 4 (b). The modified Johnson-Cook parameters for the steel material are presented in Table 1.

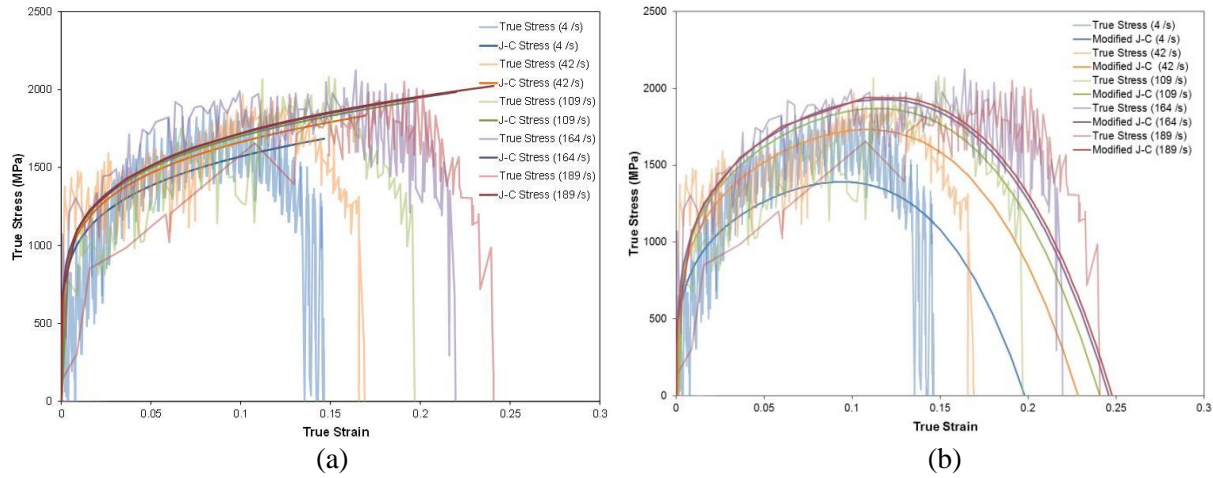


Figure 4: (a) Johnson-Cook curve fits and (b) modified Johnson Cook curve fits for Algotuf 400 steel

Table 1: Modified Johnson-Cook model curve fitting parameters for Algotuf 400 steel at room temperature

Parameter	A	B	C	n	D	p	E
Value	-0.07611	0.68260	530.95588	0.18713	-13223.66726	4.05979	0.17353

Furthermore, the results showed that the yield strength, ultimate strength, elongation at failure, and fracture energy all increased as the test strain rate increased.

## INTERMEDIATE STRAIN RATE CHARACTERIZATION OF MATERIALS USING A HIGH SPEED SERVO-HYDRAULIC LOAD FRAME

### 3.2 Aluminum

Aluminum 6061-T6 specimens were tested at strain rates ranging from static to  $156 \text{ s}^{-1}$  at room temperature as well as  $100^\circ\text{C}$ . The true stress-strain curves and modified Johnson-Cook model for the room temperature tests are shown in Figure 5. A graph showing the effects of temperature on the material behaviour at intermediate strain rates is shown in Figure 6, and the final parameters for the modified Johnson-Cook model are listed in Table 2.

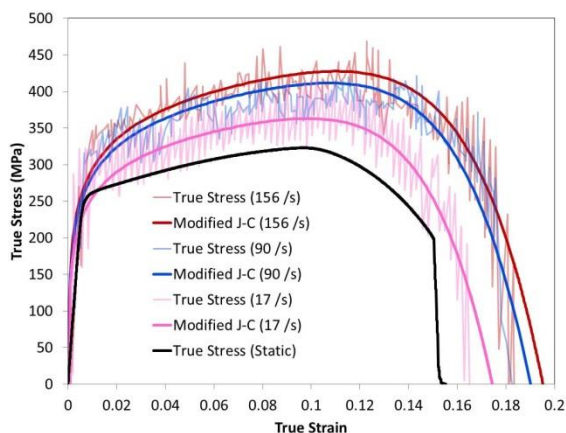


Figure 5: True stress-strain curves for Aluminum specimens at room temperature

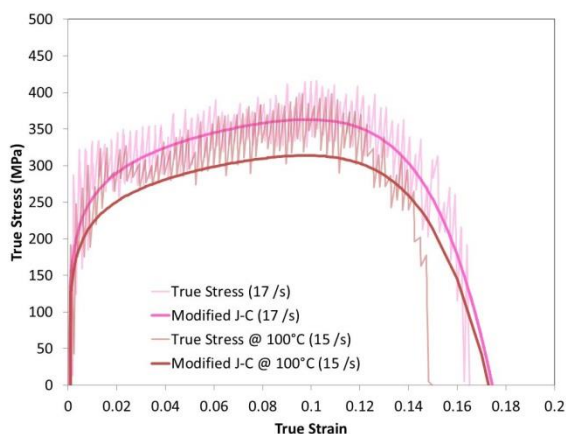


Figure 6: Comparison of true stress-strain curve and modified Johnson-Cook model for aluminum at  $100^\circ\text{C}$

Table 2: Modified Johnson-Cook parameters for Aluminum 6061-T6

Parameter	A	B	C	n	D	p	E	m
Value	-0.24006	0.24701	6265.53578	0.00263	-2956223.66726	7.05979	0.16353	0.98695

One can tell from the true stress-strain curve that for aluminum 6061-T6 the yield strength, tensile strength, and elongation at failure increase as the strain rate increases. The tests at elevated temperatures show lower strength and failure strains than those tested at room temperature. It can also be seen from Figure 6 that the modified Johnson-Cook model can reflect the strength decrease due to temperature, although the failure strain is not predicted accurately.

**INTERMEDIATE STRAIN RATE CHARACTERIZATION OF MATERIALS USING A HIGH SPEED SERVO-HYDRAULIC LOAD FRAME**

**3.3 Epoxy**

Type V dogbone tensile specimens as described in ASTM D638 [14] were made of EPON 828 epoxy resin from Hexion Inc. USA. The specimens were tested quasi-statically and up to a head velocity of 2 m/s, which corresponds to strain rates ranging from  $5.5 \times 10^{-4}$  to  $107 \text{ s}^{-1}$ . The stress-strain curves of all specimens are shown in Figure 7.

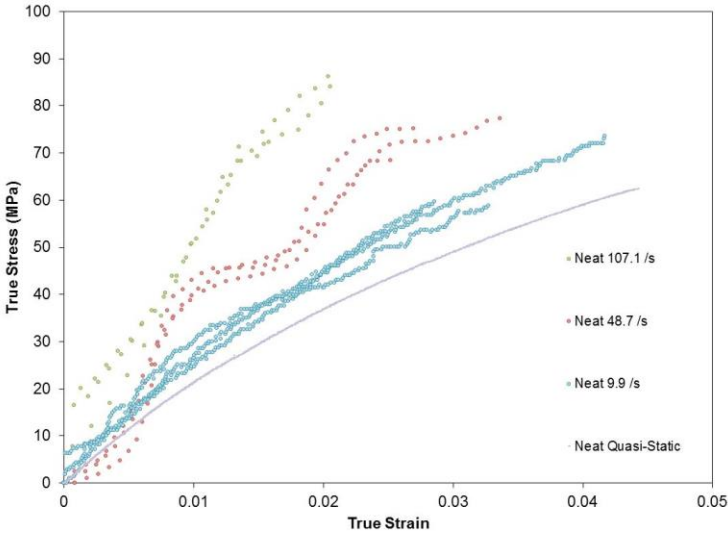


Figure 7: True stress-strain curves of epoxy specimens

Three specimens were tested for each dynamic strain rate shown in Figure 7 and it can clearly be seen that the tests yield consistent results for specimens tested at the same strain rate. From the true stress-strain curves, two material properties – ultimate tensile strength and Young’s Modulus – were investigated further and are plotted against strain rate in Figure 8. For the type of epoxy material studied, it was observed that the tensile strength and Young’s modulus increase as the strain rate increases.

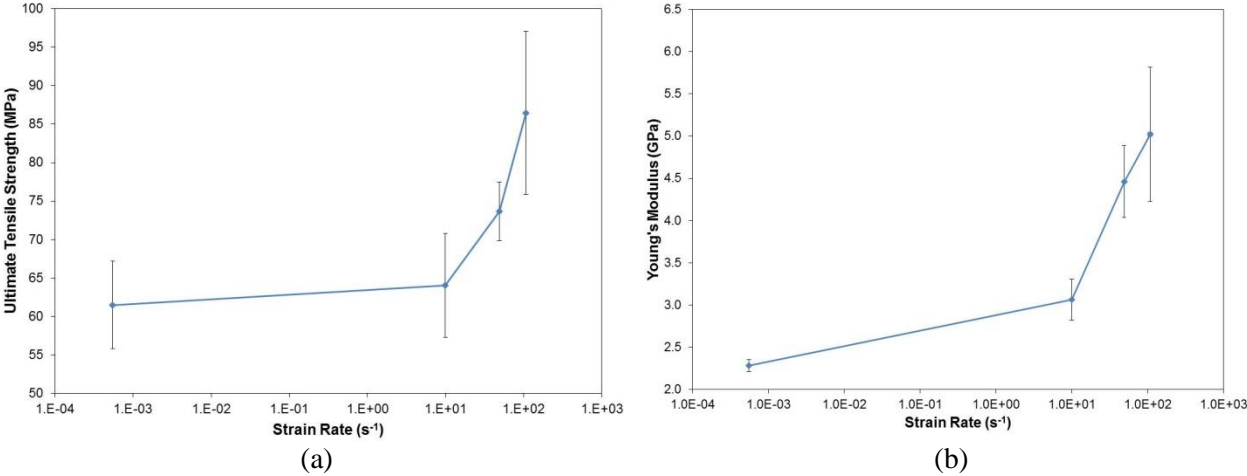


Figure 8: (a) Ultimate tensile strength, (b) Young’s Modulus

## **4 CONCLUSION**

This work presented the process used to perform tensile tests at intermediate strain rates using NRC's high speed servo-hydraulic load frame. The method of using strain gauges mounted on the tab section of the specimens was introduced as a way to circumvent the ringing caused by the sudden application of the load in the force link. A modified Johnson-Cook model was used to model the true stress-strain curves of metals at elevated strain rates. This modified model adds the capability to predict the decrease in stress and failure strain after the ultimate tensile strength has been reached. For tests at elevated temperatures the model was capable of following the decreased strength of the material. Stress-strain plots as well as modified Johnson-Cook curve-fits were produced for both steel and Aluminum, and demonstrated that the tensile strength of both metals increased as strain rate was increased. The epoxy material EPON 828 displayed strain sensitive properties as both the ultimate tensile strength and Young's modulus increased with strain rate. In conclusion, this paper displays the types and quality of tensile test results that can be achieved using a high speed servo-hydraulic load frame to test material properties at intermediate strain rates.

## **5 ACKNOWLEDGEMENTS**

Financial support by the National Research Council Canada (NRC) through the Security Materials Technology (SMT) Program is appreciated.

## **6 REFERENCES**

- [1] Y. Xia, J. Zhu, and Q. Zhou, "Verification of a multiple-machine program for material testing from quasi-static to high strain-rate," *International Journal of Impact Engineering*, vol. 86, pp. 284-294, 2015.
- [2] Y. Ou and D. Zhu, "Tensile behavior of glass fiber reinforced composite at different strain rates and temperatures," *Construction and Building Materials*, vol. 96, pp. 648-656, 2015.
- [3] M. Rahmat and S. Hind, "High Strain Rate Material characterization by High Speed Servo-Hydraulic Load Frame," National Research Council Canada, Ottawa 2016.
- [4] S.V. Hayes and D. F. Adams, "Rate sensitive tensile impact properties of fully and partially loaded unidirectional composites," *J. Test. Eval.*, vol. 10, pp. 61-68, 1982.
- [5] A. Rotem and J. M. Lifshitz, "Longitudinal strength of unidirectional fibrous composite under high rate of loading," in *26th Annual Tech. Conf., Soc. Plastics Industry, Reinforced Plastics/Composites Division*, Washington, DC, 1971, pp. 1-10.
- [6] J. Harding and L. M. Welsh, "A tensile testing technique for fibre-reinforced composites at impact rates of strain," *J. Mater. Sci.*, vol. 18, pp. 1810-1826, 1983.
- [7] K. Kawata, A. Hondo, S. Hashimoto, N. Takeda, and H. L. Chung, "Dynamic behaviour analyses of composite materials," in *Japan-US Conference on Composite Materials*, Tokyo, 1981, pp. 2-11.
- [8] S. Barre, T. Chotard, and M. L. Benzeggagh, "Comparative study of strain rate effects on mechanical properties of glass fibre-reinforced thermoset matrix composites," *Composites Part A*, pp. 1169-1181, 1996.
- [9] H. Huh, J. H. Lim, and S. H. Park, "High Speed Tensile Test of Steel Sheets for the Stress-Strain Curve at the Intermediate Strain Rate," *International Journal of Automotive Technology*, vol. 10, pp. 195-204, 2009.

**INTERMEDIATE STRAIN RATE CHARACTERIZATION OF MATERIALS USING A HIGH SPEED SERVO-HYDRAULIC LOAD FRAME**

- [10] D. Zhu, B. Mobasher, S. D. Rajan, and P. Peralta, "Characterization of Dynamic Tensile Testing Using Aluminum Alloy 6061-T6 at Intermediate Strain Rates," *Journal of Engineering Mechanics*, vol. 137, pp. 669-679, 2011.
- [11] X. Xiao, "Dynamic tensile testing of plastic materials," *Polymer Testing*, vol. 27, pp. 164-178, 2008.
- [12] Y. Xia, J. Zhu, K. Wang, and Q. Zhou, "Design and verification of a strain gauge based load sensor for medium-speed dynamic tests with a hydraulic test machine," *International Journal of Impact Engineering*, vol. 88, pp. 139-152, 2016.
- [13] D. Zhu, S. D. Rajan, B. Mobasher, A. Peled, and M. Mignolet, "Modal Analysis of a Servo-Hydraulic High Speed Machine and its Application to Dynamic Tensile Testing at an Intermediate Strain Rate," *Experimental Mechanics*, vol. 51, pp. 1347-1363, 2010.
- [14] A. International, "Standard Test Method for Tensile Properties of Plastics," vol. D638, ed, 2014.
- [15] G. R. Johnson and W. H. Cook, "Fracture characteristics of three metals subjected to various strains, strain rates, temperatures and pressures," *Engineering Fracture Mechanics*, vol. 21, pp. 31-48, 1985.
- [16] D. N. Zhang, Q. Q. Shangguan, C. J. Xie, and F. Liu, "A modified Johnson-Cook model of dynamic tensile behaviors for 7075-T6 aluminum alloy," *Journal of Alloys and Compounds*, vol. 619, pp. 186-194, 2015.
- [17] E. Corona and G. E. Orient, "An evaluation of the Johnson-Cook model to simulate puncture of 7075 aluminum plates," Sandia National Laboratories, 2014.